

NEW GLYCOGEN DERIVATIVES AS AN ADVANTAGEOUS POLYMERS CARRIER IN BACTERIA THERANOSTICS

F.J. Fadel, M.M. Kareem, F.H. Mohammed

Department of Chemistry, College of Science, University of Babylon, Babylon, 51002 Iraq Email: <u>sci.mohanad.mousa@uobabylon.edu.iq</u>

> Received 09.06.2024 Accepted 07.08.2024

Abstract: Pharmaceutical polymers based on glycogen as prodrugs were synthesized to enhance the physical and chemical properties, thereby increasing the solubility of the drugs compared to the original drugs. This improvement leads to better efficacy and bioavailability, enhancing their absorption and distribution within the body. The drug release process in prodrugs contributes to sustained pharmacological effects, extending the duration of therapeutic effects compared to immediate-release formulations. This research involves the preparation of pharmaceutical polymers [FA6-FA10] based on glycogen through the reaction of glycogen with maleic anhydride, followed by the addition of thionyl chloride and amino drugs to obtain new pharmaceutical polymers. These polymers were characterized spectrally using Fourier-transform infrared (FTIR) spectroscopy and proton nuclear magnetic resonance (¹H NMR) spectroscopy. The physical properties of the polymers, such as swelling, viscosity, and controlled drug release in acidic, basic, and neutral media, were studied. The antibacterial properties were also investigated against two types of bacteria, namely Gram-positive and Gram-negative bacteria, using the disk diffusion technique. The results were compared with corresponding antibacterial drugs, indicating an increase in the antibacterial activity of the pharmaceutical polymers.

Keywords: Pharmaceutical polymers, glycogen, maleic derivative, antibacterial activity, drug release.

DOI: 10.32737/2221-8688-2025-2-166-177

Introduction

Pharmaceutical polymers are employed in enhancing drug delivery techniques, including oral vaccination. These polymers facilitate the effective and safe transport of medications, thereby contributing to the treatment infectious diseases through oral vaccination [1]. effectively Drugs are delivered using pharmaceutical polymers, which demonstrate high efficacy in combating tumors with different toxicity levels compared commercial formulations [2]. These polymers enable effective release and targeted delivery of formulated medications drugs, with the exhibiting high stability, increased solubility, enhanced bioavailability, and reduced side effects. Biodegradable polymers are employed in pharmaceutical formulations due to their ability to degrade within the body, thereby reducing dosing frequency and improving patient safety [3].

Drug carriers are biocompatible materials

used in pharmaceutical, cosmetic, and food applications for transporting molecules. Drug carriers are classified based on their shape, geometry, and production methods, such as liposomes, isothiozomes, and aquasomes. They have applications in medical fields such as cancer treatment, antiviral therapy, and gene therapy [4]. There are specialized mechanisms for pharmaceutical carriers such as nanoparticles, liposomes, and hydrogel formulations with controlled compositions and structures. Some polyelectrolytes are distinguished by their ability to deplete ATP, thereby inhibiting the function of glycoproteins and preventing tumors from developing resistance to multiple drugs [5, 6].

Glycogen can form strong and flexible hydrogels due to its hydrogen bonding capabilities and interactions with metals, which grant the hydrogels excellent self-healing abilities. Additionally, it can be used to prepare cohesive films that promote cellular adhesion and proliferation, making it valuable in tissue engineering applications [7]. Glycogen is biocompatible and biodegradable, making it suitable for use in polymer carriers for medical applications. Glycogen-based compounds have the ability for imaging and tumor targeting, and their accumulation in tumors facilitates their visualization using MRI and crystallographic imaging techniques [8]. Glycogen is similar to starch but is inert and stable against amylase activity, maintaining stability when administered intravenously [9-11].

Drug absorption begins with oral ingestion, where drugs pass from the esophagus to the stomach. In the stomach, drugs encounter acidic conditions that may degrade them.

Subsequently, drugs move to the intestines where they are further broken down and absorbed [12-14]. Drug distribution occurs throughout the body following drug absorption, as they are transported to various tissues and organs. This distribution happens seamlessly through the circulatory system, delivering drugs to their targeted sites where they exert their therapeutic effects [15]. Drug distribution within tissues is influenced by their polarity, which impedes their ability to traverse cell membranes. Lipophilic drugs, however, can readily diffuse across cell membranes and distribute throughout the body upon reaching their targeted site. Drug metabolism involves metabolic processes within the body that break down and eliminate drugs.

Scheme 1. General scheme for Synthesis of compounds (FA6-FA10) and used model drug molecules

Chemical reactions in metabolism convert drugs into different compounds that can be easily excreted [14-17].

Swelling this mechanism involves the expansion of water-absorbing polymer carriers upon contact with water, triggering drug release as the polymer swells [18]. Proper control of polymer swelling is crucial for regulating drug release kinetics [19, 20]. There are broad-spectrum antibiotics that target specific strains

of bacteria, including Gram-positive and Gramnegative bacteria [21, 22], Therefore, they offer a comprehensive approach to treating infections from various bacterial strains [23-28].

Here, we are developing the novel pharmaceutical polymers with biological activity by combining maleic anhydride and glycogen, then reacting with five medications that include amines (Scheme 1).

Experimental part

Materials and characterization

Analytical-grade solvents and reagents were sourced from Fluka, Sigma-Aldrich, CDH, and Riedel-deHaen for the purposes of analysis. SDI-Samarra Company supplied sulfadiazine, mefenamic acid, trimethoprim, and benzocaine. Fourier Transform Infrared (FTIR) spectra were captured using a Bruker Tensor II Fourier Transform Infrared Spectrometer. The ATR-FTIR spectra were recorded in the range of 400 to 4000 cm⁻¹ employing a Bruker Tensor II Transform Infrared Fourier Spectrometer Promoter ATR-FTIR. Melting points were determined using an SMP30 melting point apparatus. The densities of polymer solution samples were measured at 23°C using a METTLER TOLEDO Densito 30px Portable Density Meter. The viscosity (n) of the synthesized polymers in acetone at 23°C was determined using an Ostwald viscometer. UV absorbance was measured with a PG CECIL-CE7200 double-beam spectrophotometer. ¹H NMR spectra were acquired on a Varian INOVA 500 MHz NMR spectrometer in dimethyl sulfoxide (DMSO-d6), with TMS serving as the reference standard, and chemical shifts expressed in parts per million (ppm).

General Procedure for the synthesis of FA6-FA10 polymer derivatives

In 10 mL of dimethyl sulfoxide (DMSO), one gram of glycogen (one mole) was dissolved, and in 5 milliliters of DMSO, 0.45 grams of maleic anhydride (three moles) were dissolved. Following that, the aforementioned solutions were combined in 100 mL conical flasks and heated to 70 °C under nitrogen for an hour in order to produce an orange gelatinous solution. To get acetyl chloride, the reaction mixture was stirred continuously (with a magnetic stirrer) for 30 minutes while ten drops of SOCl₂ were added. Afterwards, the reaction mixture was treated with ten drops of triethylamine to eliminate any remaining chlorine. After adding 2.483 grams (3 moles) of (carvingdilol, Sulfanilamide, procaine hydrochloride, amoxicillin, and 4-aminoantipyrine), the boiling process was carried out for an hour at 70 °C under nitrogen, while stirring continuously. To allow the solid particles to precipitate, the mixture was then submerged in ice. Following a two-day, it was washed with ethanol and acetone to remove impurities, and then rinsed with ether to eliminate any remaining moisture before being allowed to dry. The intrinsic viscosity of these polymers was measured using an Ostwald viscometer [23, 24].

Table 1. Physical properties of polymers FA6-FA10.

Polymer	Color	m.p °C
FA6	Brown	195-197 ° C
FA7	light brown	155-160 °C
FA8	Dark red	130-132 ° C
FA9	Dark red	135-139 ° C
FA10	Black	111-115 °C

The biological activity of the prepared polymers against both positive and negative bacteria was studied and compared with pure drugs. The following Table 1 describes the resulting compounds.

Polymer swelling ratio Analysis: To study

how the drug-loaded polymers swelled, we used a small amount (0.2 g), using a pure water at 25 °C as the swelling medium [25-27]. After 48 hours, the samples were taken out, and their weight was recorded both before and after they swelled.

Swelling ratio =
$$\frac{W_s - W_d}{W_d} \times 100$$

Where, W_S = weight of swelling polymer, gr, W_d = weight of polymer, gr.

Results and discussion

A new pharmaceutical polymers based on glycogen derivative was produced in good yield by condensation with several drugs, including Sulfanilamide, procaine hydrochloride, amoxicillin. 4-aminoantipyrine. and produced compounds were examined using a variety of analytical methods, including ¹H NMR, and FTIR. Escherichia coli (E. coli) and Staphylococcus aureus (S. aureus) were the two gram-positive and gram-negative bacteria used to test the antibacterial activity of the produced derivatives [29-31].

For polymer FA6 the ¹HNMR spectrum shows: CH-NH 5.9 ppm; N-CH 2.97 ppm; (Ar) CH=CH 6.84-6.98 ppm; O-CH 4.07 ppm; HO-CH 3.6-3.9 ppm; O-CH₂ 4.13-4.38 ppm; CH=CH (Alph.) 6.22-6.27 ppm. FTIR spectrum shows: CH₃- 2869.88-2988 cm⁻¹; OH- 3259.06 cm⁻¹; new C=O amide group at 1640 cm⁻¹and disappearing of –OH carboxyl group of glycogen maleic derivative: CH=CH (Alph.) 1582.29 cm⁻¹; CH=CH (Ar) 1502.58-1454 cm⁻¹ (Fig.1).

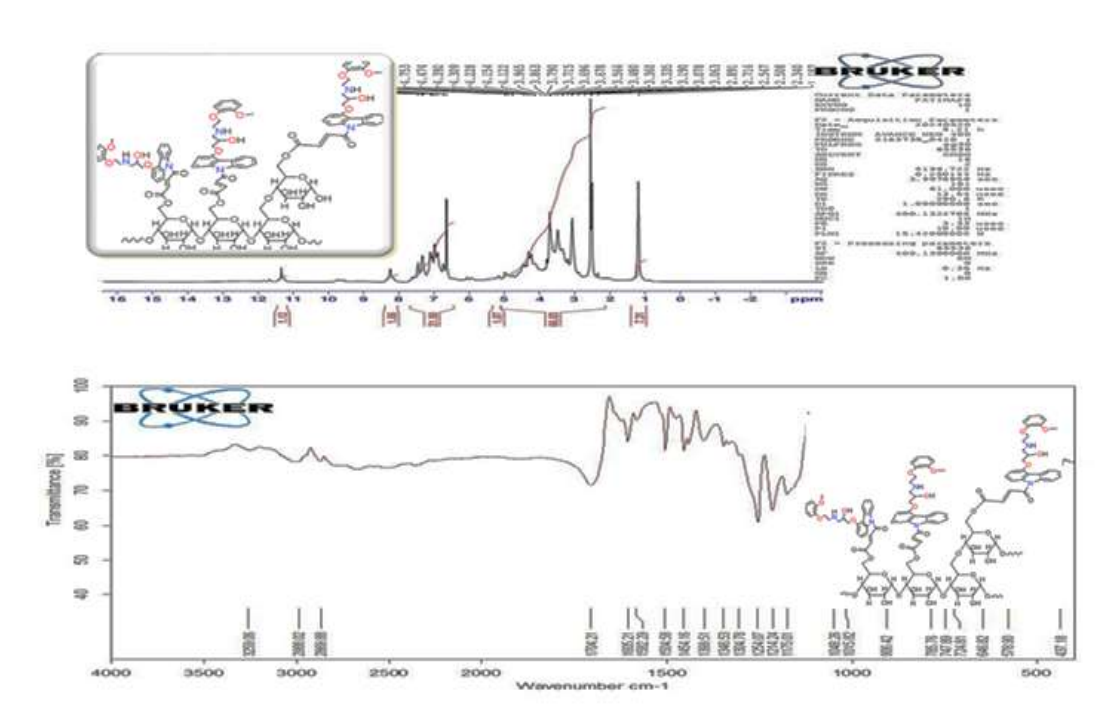


Fig. 1. ¹H NMR and FTIR spectra of FA6 polymer derivative

¹HNMR spectrum of polymer FA7 shows: SO₂-NH₂ 6.89 ppm; C=CH Aromatic 7.64-7.70 ppm; CO-NH- 9.82 ppm; C=CH 6.22-6.27 ppm; COO-CH₂ 4.38-4.14 ppm; OH-CH 3.6-3.9 ppm;

CH-OH 4.70-4.88 ppm; O-CH 4.19 ppm. FTIR spectrum shows: appearing amide C=O at 1643 cm⁻¹ and disappearing of –OH carboxyl group of glycogen maleic derivative; C=C aliphatic 1602

cm⁻¹; OH 3342 cm⁻¹; C=C Aromatic 1535 cm⁻¹; NH₂ 3232 cm⁻¹, 3240 cm⁻¹; SO₂ 1153-1089 cm⁻¹ (Fig.2).

Polymer FA8 the ¹H NMR spectrum shows :CH=CH 7.84 ppm; CHN-CH₃ 1.14 ppm; CO-NH 10.02 ppm; COOCH₂ 4.30 ppm; N-CH₂ 2.79-2.89 ppm; CH=CH 6.22-6.27 ppm; HO-CH 3.6-3.9 ppm; CH-OH 4.71-4.88 ppm; -O-

CH 5.4-5.3 ppm. FTIR spectrum shows new C=O amide group at 1643.41 cm⁻¹ and disappearing of –OH carboxyl group of glycogen maleic derivative; appearing C=O ester 1751.13 cm⁻¹; C=C aliphatic 1602.90 cm⁻¹ C=C Aromatic 1570 cm⁻¹, 1516 cm⁻¹; C-O-C ether 1369-1271 cm⁻¹; =C-H Aromatic 3076 cm⁻¹; C-H Aliphatic 2808-2889 cm⁻¹ (Fig.3).

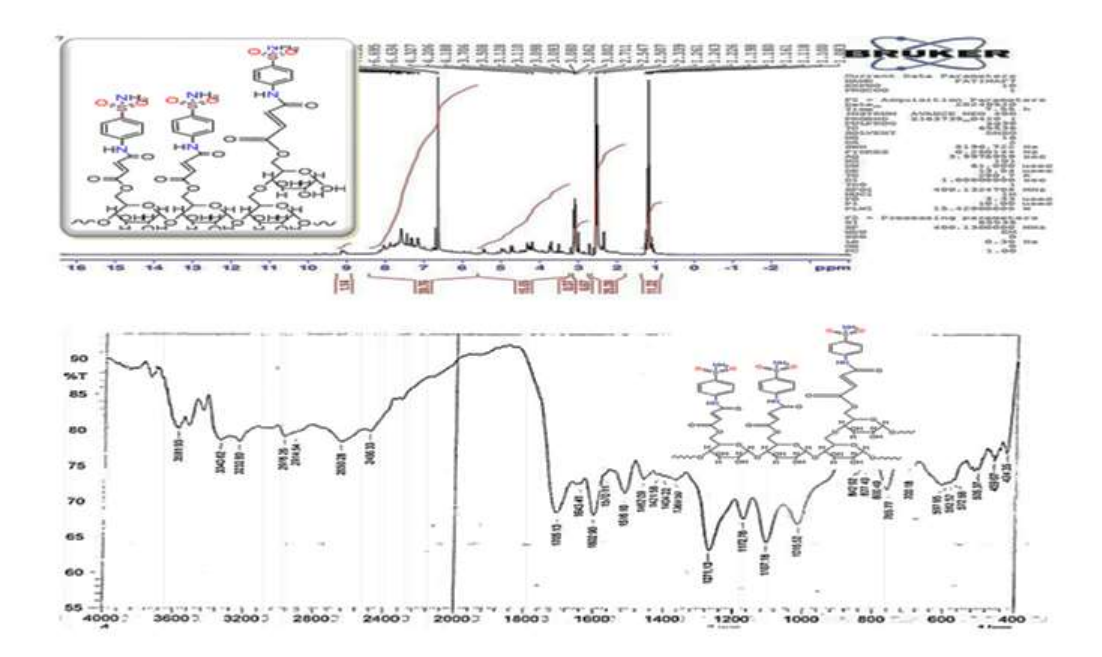


Fig. 2. ¹H NMR and FTIR spectra of FA7 polymer derivative

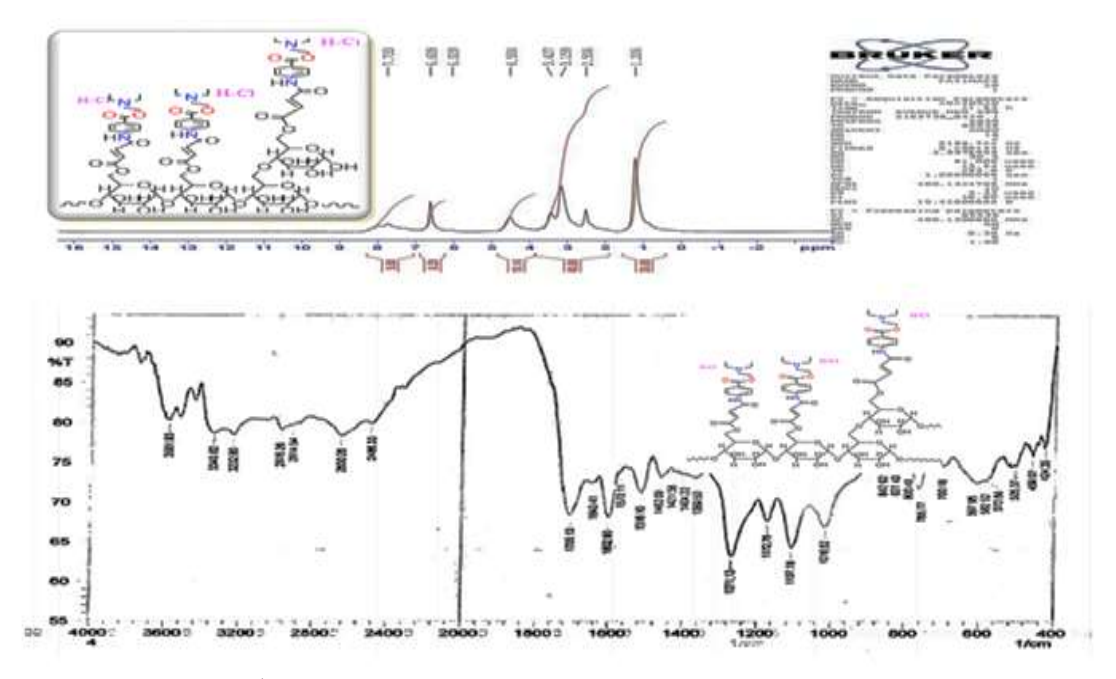


Fig. 3. ¹H NMR and FTIR spectra of FA8 polymer derivative

Polymer FA9 the ¹H NMR spectrum shows: N-CH 4.54 ppm; S-CH 4.86 ppm; CH₃-1.55 ppm; CO-NH 8.32-9.13 ppm; Ar-OH 9.08 ppm, CH=CH (Ar) 6.71-6.99 ppm; CH=CH

(Alph.) 6.22-6.27 ppm; COOCH 4.13-4.38 ppm; CH-OH 4.32-4.71 ppm; O-CH 5.30-5.70 ppm; OH-CH 3.70-3.88 ppm; OH carboxyl 11.5-12.3 ppm. FTIR spectrum shows: new CO-NH

1613.61 cm⁻¹; CH=CH (Alph.) 1516.74 cm⁻¹; CH=CH (Ar) 1480-1416 cm⁻¹; C=O carboxyl 1715 cm⁻¹; OH carboxyl 2500-3400 cm⁻¹ (Fig.4).

The ¹H NMR spectrum of the FA10 polymer shows: CH=CH (Ar) 7.35-7.52 ppm; N-CH₃- 3.10 ppm; CH=CH (Alph.) 6.22-6.27 ppm; CO-NH 9.86 ppm; CH=CH-CH₃ 2.18

ppm; O-CH 4.19 ppm; HO-CH 3.6-3.9 ppm; CH-OH 4.71-4.88 ppm; COOCH₂ 4.14-4.38 ppm. FTIR spectrum shows: shows new C=O amide group at 1656.06 cm⁻¹and disappearing of –OH carboxyl group of glycogen maleic derivative; CH=CH (Alph.) 1591.32 cm⁻¹; CH=CH (Ar) 1490-1421 cm⁻¹, -CH₂ 2872.09 - 2982.11 cm⁻¹; C=O amide 1650 cm⁻¹ (Fig. 5).

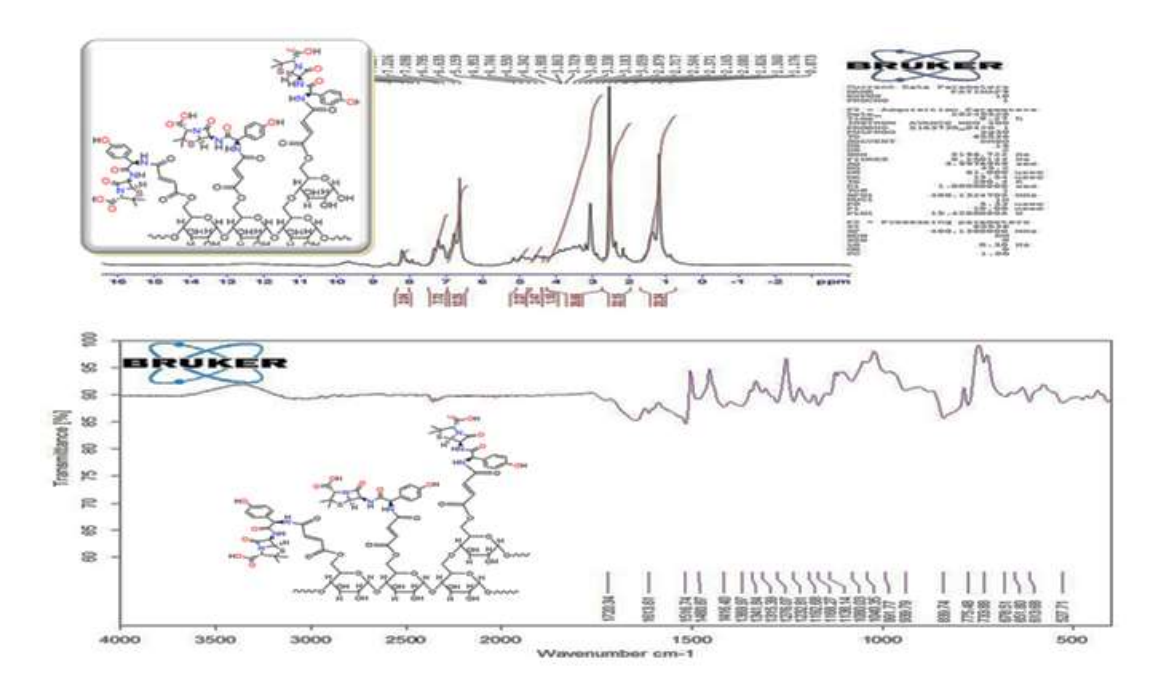


Fig. 4. ¹H NMR and FTIR spectrum of FA9 polymer derivative

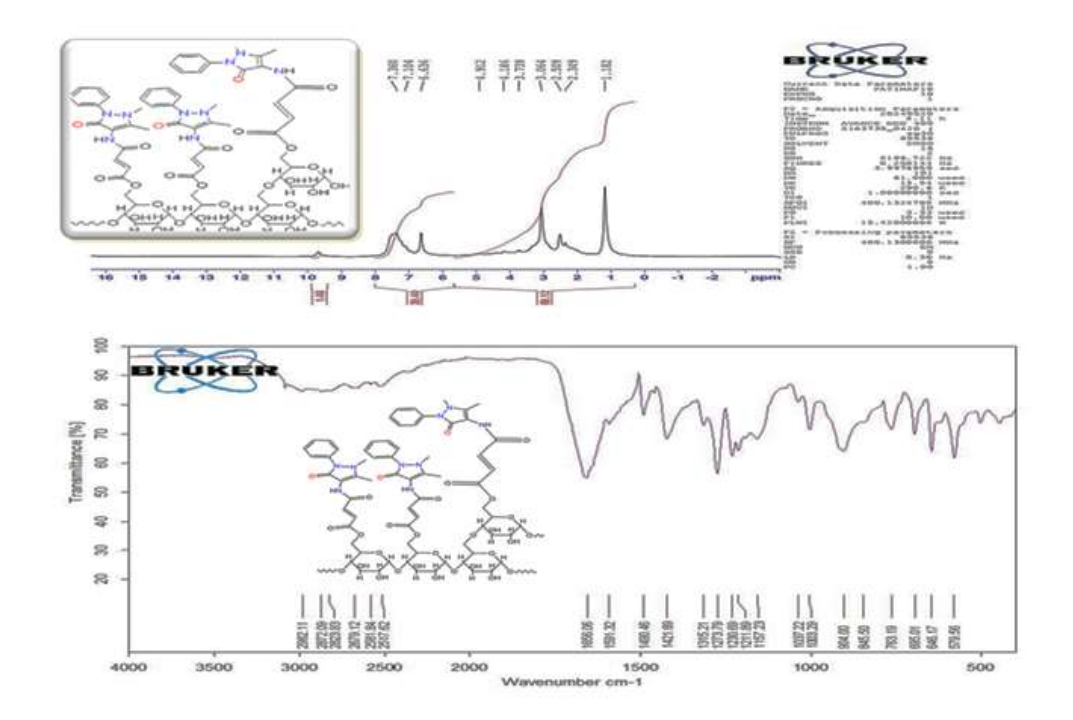


Fig. 5. ¹H NMR and FTIR spectrum of FA10 polymer derivative

Amides with low molecular weights are less soluble in water due to their limited ability to form hydrogen bonds with water molecules. Similarly, solubility increases as the branching of the polymer chain increases. This is because the branches reduce the surface area of the non-polar hydrocarbon segments, thus increasing

solubility. The molecules in the solute and nonpolar solvent can only exert dispersion forces on one another. There is virtually little energy released by this. Thus, altogether, solubility won't occur since more energy is needed than is released (Table 2).

Table 2. Solubility of the polymers FA6-FA10

Polymer	H ₂ O	EtOH	MeOH	CHCl ₃	Hexane	Diethyl	Acetone	Ethyl	DMSO	DMF	Toluene	Dioxane
						ether		acetate				
FA6	P.	P.	+	P.	-	-	+	-	+	+	-	+
FA7	P.	-	P.	-	-	-	P.	-	+	+	P.	-
FA8	+	P.	P.	-	-	-	P.	-	+	+	-	+
FA9	P.	-	P.	-	-	-	+	-	+	+	-	+
FA10	+	-	P.	-	-	-	+	-	+	+	-	P.

*P.=Partial

Table 3 data explain that Swelling occurs when polymer molecules penetrate between solvent molecules. It is observed that the FA10 sample exhibits greater swelling compared to other samples, which is attributed to its higher molecular weight. As the molecular weight of the pharmaceutical polymer increases, its capacity to carry the drug and its ability to swell both increase. This results in a faster drug release, as the bond between the polymer and the drug weakens until it breaks and the drug is released. In contrast, the FA9 polymer exhibits the least swelling. The swelling ratio of drug polymer derivatives as follows: FA6 18.5%, FA719 %, FA8 19.5%, FA9 17 %, FA10 19.8 %.

Viscometer measures intrinsic viscosity

and uses the Mark-Houwink equation to determine viscosity-average molecular weight. The equation describing the dependence of the intrinsic viscosity of a polymer on its relative molecular mass (molecular weight) is: $[\eta]=KM^a$, where $[\eta]$ is the intrinsic viscosity, K and α are constants the values of which depend on the nature of the polymer and solvent as well as on temperature, and M is usually one of the relative molecular mass averages.

The FA6 sample exhibits higher viscosity compared to the other prepared polymers due to its high molecular weight (Tables 3-7). There is a direct relationship between molecular weight and viscosity, as described by the Mark-Houwink equation.

Table 3. Data of FA6 used to determine the intrinsic visco	sity
---	------

FA6 polymer concentration, mg/ml	Time flow t/s	$\eta/\eta_o=t/t_o$	$\eta_{red} = \eta_{sp}/C$
Acetone	43	1	0
2	56.38	1.3112	0.1556
4	71	1.65488	0.16372
6	86.73	2.01718	0.16953
8	104.28	2.42528	0.17816
10	122.14	2.8406	0.18406
$[\eta] = 0.163$	$M_{\eta} = 5085.97$		

Table 4. Data of FA7 used to determine the intrinsic viscosity

FA7 polymer concentration, mg/ml	Time flow t/s	$\eta/\eta_o=t/t_o$	$\eta_{\text{red}} = \eta_{\text{sp}}/C$
Acetone	43	1	0

10 [ŋ] = 0.1389	104.31 $M_{\eta} = 4183.19$	2.426	0.1426
8	91	2.120928	0.140116
6	78.6	1.82824	0.13804
4	66.18	1.55392	0.1348
2	54	1.26368	0.131844

Table 5. Data of FA8 used to determine the intrinsic viscosity

FA8 polymer concentration, mg/ml	Time flow t/s	$\eta/\eta_o=t/t_o$	$\eta_{\text{red}} = \eta_{\text{sp}}/C$
Acetoe	43	1	0
2	55.73	1.2961	0.14805
4	68.63	1.5962	0.14905
6	81	1.9042	0.1507
8	95.54	2.22192	0.15274
10	109.22	2.54	0.154
$[\eta] = 0.149$	$M_{\eta} = 4584.87$		

Table 6. Data of FA9 used to determine the intrinsic viscosity

FA9 polymer concentration, mg/ml	Time flow t/s	$\eta/\eta_o=t/t_o$	$\eta_{red} = \eta_{sp}$ /C
Acetone	43	1	0
2	54.5	1.2688	0.1344
4	66.59	1.548836	0.137209
6	79	1.84138	0.14023
8	92.66	2.15496	0.14437
10	106.64	2.4801	0.148116
$[\eta] = 0.143$	M_{η} =4362.76		

Table 7. Data of FA10 used to determine the intrinsic viscosity

FA10 polymer concentration, mg/ml	Time flow t/s	$\eta/\eta_o=t/t_o$	η _{red} =η _{sp} /C
Acetone	43	1	0
2	54.87	1.27618	0.13809
4	67	1.560464	0.140116
6	80	1.86046	0.14341
8	93	2.17952	0.14744
10	107.38	2.4974	0.14974
$[\eta] = 0.1468$	M_{η} =4476.28		

Multiple factors impacting the positions of bands in the UV spectrum can relate to variations in drug release rates. Among these effects, the most significant is the conjugation effect, which results in a red shift due to chain elongation, including conjugated bonds. As energy levels get closer, electronic transitions to vacant molecular orbitals require less energy. Greater conjugation leads to a higher maximum wavelength .This suggests that drug release

takes six days and is faster in basic than acidic media. The hydroxide ion targets the carbon atom of the carbonyl group with greater nucleophilicity than either the proton or the water molecule. Various elements, such as the kind of bond (the ester or amide), the extent of swelling, the characteristics of the drug, and the level of crosslinking within polymer chains, influence the rate of drug release. Crosslinking decreases both the drug release rate and the

extent of polymer swelling. Figure 6 indicates that the drug release process was studied in three different media (acidic, basic, and neutral), where hydrolysis occurs, leading to the release of the drug from the sample. The findings indicate that the drug release process concludes

after six days, and that controlled drug release in the basic medium is faster than in the acidic medium. This is because the nucleophilic attack of the hydroxide ion on the carbonyl group is more effective than that of the proton or water molecule.

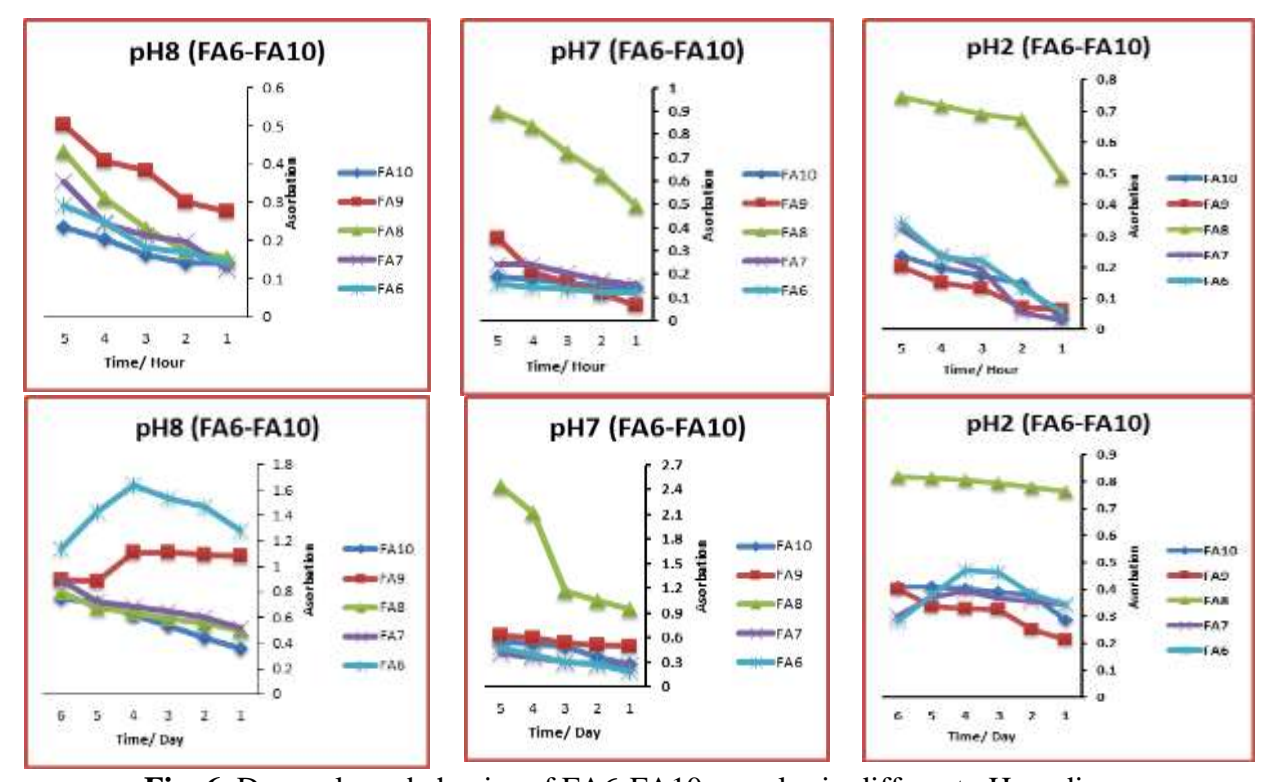


Fig. 6. Drug release behavior of FA6-FA10 samples in different pH medium.

Table 8. Antibacterial activity of synthesized polymers-drug derivatives

Sample	Inhibition zone for staphylococcus of polymer (mm)	Inhibition zone for E.coli of polymer (mm)	Drugs	Inhibition zone for staphylococcus of Drug (mm)	Inhibition zone for E.coli of Drug (mm)
FA6	4	8	Carvedilol	30	3
FA7	5	10	Sulfanilamide	4	5
FA8	6	8	Procaine HCl	4	3
FA9	5	15	Amoxicillin	25	6
FA10	8	8	4-	4	3
			Aminoantipyrine		

The results according to Table 8 shows that FA7, FA8 and FA10 have a good inhibition zone (5, 6 and 8 mm) against S. aureus and (10, 8 and 8 mm) against E. coli in comparison to used drugs inhibitions. While, good inhibition of growth for homopolymers FA6 and FA9 against bacteria with higher effect toward E. coli. Most of the prepared compounds using

DMSO (0.1 mg/ml) showed exhibit higher antibacterial activity against Gram-negative bacteria (*E. Coli*) than against Gram-positive bacteria. This increased activity may be due to the lipophilic nature of maleimide, which enables it to permeate the lipid-rich outer membrane of Gram-negative bacteria.

Conclusion

Pharmaceutical polymers with biological activity were synthesized by reacting glycogen with maleic anhydride, followed by reaction with five amine drugs. After preparation, these polymers were characterized spectrally which provided distinct signals indicative of the formation of the target molecules from the starting materials. The physical properties of these pharmaceutical polymers were studied. Controlled drug release was investigated in three different media (pH 8, pH 7, pH 2), and it was found that these polymers exhibit complete release in basic medium. The solubility of the prepared polymers was studied in various organic solvents, revealing higher solubility in

polar solvents. The biological activity of these polymers was also assessed, and it was found that most of them exhibit higher activity against Gram-negative bacteria (E.coli) compared to Gram-positive bacteria (Staphylococcus aureus). The viscosity of these pharmaceutical polymers was measured using acetone as the solvent and an Ostwald viscometer. The results indicated varying viscosity values, suggesting that solvent molecules penetrate the polymer chains. Additionally, the swelling behavior of the polymers was studied using water over 48 hours at 25 °C, and it was found that the polymer layers swell due to water saturation but do not dissolve.

References

- 1. Jana P., Shyam M., Singh S., Jayaparakash V., Dev A. Biodegraddable polymer in drug delivery and oral vaccination. *Our. Polym. J.* 2021, Vol. **142**, 110155.
- 2. Diez-pascual A.M. Synthesis and applications of biopolymer composites. *Int. J. Mol. Sci.* 2019, Vol. **20**(9), p. 2321
- 3. Raja D.K., Pager D.D., Menezes P.L., Linul E. Fiber-reinforced polymer composites: Manufacturing, properties, and applications. *Polymers (Basel)*. 2019, Vol. **11(10)**, 1667.
- 4. Trujillo P. Drug Carriers: Classification, Administration, Release Profiles, and Industrial Approach. *Processes*, 2021, Vol. **9(3)**, 470.
- 5. Yu J., Qiu H., Yin S., Wang H., Li Y. Polymeric drug delivery systems based on pluronics for cancer treatment. *Molecules*, 2021, Vol. **26(12)**, 3610.
- 6. Finbloom J.A., Sousa F., Stevens M.M., Desai T.A. Engineering the drug carrer biointererface to overcome biological barriers to drug delivery. *Adv.Drug Deliv. Rev.* 2020, Vol. **167**, p. 89—108.
- 7. Pesford Q.A., Cavalieri F., Caruso F. Glycogen as a Building Block for Advanced Biological Materials. *Adv. Mater.* 2020, Vol. **32(18)**, 1904625.
- 8. Gálisová A., Jiratova M., Rabyk M., Sticova E., Hajek M., Hruby M., Jirak D. Glycogen as an advantageous polymer carrier in cancer Theranodtics: Straightforward in vivo

- evidence. Sci. Rep. 2020, Vol. 10, 10411.
- 9. Shafiq F., Mahmood A., Ahmad A., Ashraf M., Iqbal M., Raza S.H. Glycogen-pased bionanocomposites. Bionanocomposites Green Synth. Appl. Micro and Nano Technologies. 2020, Chapter 11, p. 259-266
- Wang L., Liu Q., Tan X., Wang Z., Wang M., Wise M.J., Li Ch., Ma Ch., Li E., Deng B., Du Y., Tang D., Gilbert R.G. Molecular Structure of Glycogen in Escherichia coli. *Biomacromolecules*, 2019, Vol. 20(7), p. 2821—2829.
- 11. Dienel G.A., Carlson G.M. Magor Advances in Brain Glycogen Research: Understanding of the Roler of Glycogen Have Evolved from Emergency Fuel Reserve to Dynamic, Regulated Participant in Diverse Brain Functions. *Advances in Neurobiology*, 2019, Vol. 23, p. 1-16. doi: 10.1007/978-3-030-27480-1_1.
- 12. Senekowitsch S., Schick P., Abrahamsson В., Augustijns P., Gießmann Lennernäs H., Matthys Ch., Marciani L., Pepin X., **Perkins** A., Feldmüller M., Sulaiman S., Weitschies W., Wilson C.G., Corsetti M., Koziolek M. Application of In Vivo Imaging Techniques and Diagnostic Tools in Oral Drug Delivery Research. Pharmaceutica, 2022, Vol. 14(4), 801. doi: 10.3390/pharmaceutics14040801.

- 13. Forsberg J., Bedard E., Mahmoud S.H. Bioavailability of Orally Administered Drug in Critically II1 Patients. *J. Pharm. Practice*. 2013, Vol. **36(4)**, 967—979. doi: 10.1177/08971900221100205
- Macheras P., Chryssafidis P. Correction to: Revising Pharmacokinetics of Oral Drug Absorption: I Models Based on Biopharmaceutical/Physiological and Finite Absorption Time Concepts. *Pharm. Res.* 2020, Vol. 37(10), 187. doi: 10.1007/s11095-020-02894-w.
- 15. Bereda G. What the Body Does to A Drug: Pharmacokinetics. *Clin. Endocrinol. Metab.* 2022, Vol. 1, p. 01-09.
- 16. Mannan A., Unnisa F. Role of biochemicals and other factors affecting biotransformation and drug absorption. *Pharma Innov. J.* 2019, Vol. **8(3)**, p. 198—206.
- 17. Forester K.I., Hermann S., Mikus G., Haefeli W.E. Drug—Drug Interactions with Direct Oral Anticoagulants. *Clin. Pharmacokinet*. 2020, Vol. **59(12)**, 1647. doi: 10.1007/s40262-020-00954-3.
- 18. Moradi Kashkooli F., Soltani M., Souri M. Controlled anti-cancer drug release through Advanced nano-drug delivery systems: Static and dynamic targeting strategies. *J. Control. Release*. 2020, Vol. **327**, p. 316—349. doi.org/10.1016/j.jconrel.2020.08.012
- 19. Mahmood D.A., Kareem M.M., Witwit I.N. New n-substituted itaconimide polymers: synthesis, characterization and biological activity. *Eurasian Chem. Commun.* 2023, Vol. **5(9),** p. 866-884. doi.org/10.22034/ecc.2023.397194.1643
- Butler M.S., Gigante V., Sati H., Paulin S., Al-Sulaiman L., Rex J.H., Fernandes P., Arias C.A., Paul M., Thwaites G.E., Czaplewski L., Alm R., Lienhardt Ch., Spigelman M., Silver L.L., Ohmagari N., Kozlov R., Harbarth S., Beyer P. Analysis of the Clinical Pipeline of Treatments for Drug-Resistant Bacterial Infections: Despite Progress, More Action Is Needed. *Antimicrob. Agents Chemother.* 2022, Vol. 66(3), e0199121. doi: 10.1128/AAC.01991-21.
- 21. Mubarak H.A., Thejeel K.A., Karhib M.M., Kareem M.M. Synthesis, characterization, and evaluation of antibacterial and

- antioxidant of 1, 2, 3-triazole, and tetrazole derivatives of cromoglicic. *Eurasian Chem. Commun.* 2023, 5, p. 691-700.
- 22. Kadhim T.S., Kareem M.M., Atiyah A.J. Synthesis, Characterization And Investigation Of Antibacterial Activity For Some New Functionalized Luminol Derivatives. *Bulletin of the Chemical Society of Ethiopia*, 2023, Vol. **37(1)**, p. 159—169
- 23. Mubarak H.A., Hussein A.A., Jawad W.A.J., Karhib M.M., Alrazzak N.A., Kareem M.M., Naje A.S. Synthesis and characterization of new 4,6-dimthoxy-1H-indole derivatives as antibacterial and antitumor agents. *Aurasian Chem. Commun.* 2023, Vol. 5(5), p. 411-424.
- 24. Mubarak H.A., Thejeel Kh.A., Karhib M.M., Kareem M.M. Synthesis, characterization, and evaluation of antibacterial and antioxidant activity of 1, 2, 3-triazole, and tetrazole derivatives of cromoglicic aid. *Eurasian Chem. Commun.* 2023, Vol. **5(8)**, p. 691-700.
- 25. Kareem M.M., Nour A., Saadon A., Nagham M.A. Synthesis, Characterization and Biological activity study for new hybrid polymers by grafting 1, 3, 4-triazole and 1, 2, 4-oxadiazle moieties onto polyvinyl chloride. *Egypt J Chem.* 2021, Vol. **64(3)**, p. 1273-1284.
- 26. Shakir Z.M., Kareem M.M., Al-Baiati M.N. Study the effects of some nano graft copolymer-drugs on the spread of breast cancer. *AIP Conference Proceedings*, 2023, Vol. 2414, 050005. doi.org/10.1063/5.0114710
- 27. Shakir Z.M., Kareem M.M., Al-Baiati M.M. Inhibition of spread of the breast cancer by using of some nano co-polymer-drugs. *AIP Conference Proceedings*, 2023, 2414, 050047. doi.org/10.1063/5.0114719.
- 28. Altemus M.A., Goo L.E., Little A.C., Yates J.A., Cheriyan H.G., Wu Z.F., Merajver S.D. Breast cancer utilize hypoxic glycogen stores via PYGB, the brain isoform of glycogen phosphorylase, to promote metastatic phenotypes. *PLoS One*, 2019, Vol. **14**(9), e0220973. doi: 10.1371/journal.pone.0220973
- 29. Tapdiqov Sh.Z. Designing Poly-N-Vinylpyrrolidone based hydrogel and

- applied Higuchi, Korsmeyer-Peppas, Hixson-Crowell Kinetic models for controlled release of Doxorubicin. *Chemical Problems*, 2020, Vol. **18(2)**, p. 207-213.
- 30. Tapdigov Sh.Z. The bonding nature of the chemical interaction between trypsin and chitosan based carriers in immobilization process depend on entrapped method: A
- review. International Journal of Biological Macromolecules, 2021, Vol. **183**, p. 1676-1696.
- 31. Tapdiqov S.Z. Electrostatic and Hydrogen Bond Immobilization of Trypsine onto pH-Sensitive N-Vinylpyrrolidone and 4-Vinylpyridine Radical co-Grafted Chitosan Based on Hydrogel. *Macromol. Res.* 2021, Vol. **29**, p. 120–128.